Effects of Wood Flour and MA-EPDM on the Properties of Fused Deposition Modeling 3D-printed Poly Lactic Acid Composites

Sang-U Bae,[a] Young-Rok Seo,[a,b] Birm-June Kim,[a,*] and Min Lee [c]

Fused deposition modeling (FDM) 3D printing technology is the most common system for polymer additive manufacturing (AM). Recent studies have been conducted to expand both the range of materials that can be used for FDM and their applications. As a filler, wood flour was incorporated into poly lactic acid (PLA) polymer to develop a biocomposite material. Composite filaments were manufactured with various wood flour contents and then successfully used for 3D printing. Morphological, mechanical, and biodegradation properties of FDM 3D-printed PLA composites were investigated. To mitigate brittleness, 5 phr of maleic anhydride grafted ethylene propylene diene monomer (MA-EPDM) was added to the composite blends, and microstructural properties of the composites were examined by scanning electron microscopy (SEM). Mechanical strength tests demonstrated that elasticity was imparted to the composites. Additionally, test results showed that the addition of wood flour to the PLA matrix promoted pore generation and further influenced the mechanical and biodegradation properties of the 3D-printed composites. An excellent effect of wood flour on the biodegradation properties of FDM 3D-printed PLA composites was observed.

Keywords: 3D printing; Wood flour; MA-EPDM; Poly lactic acid; Fused deposition modeling

Contact information: a: Department of Forest Products and Biotechnology, Kookmin University, Seoul 02707, South Korea; b: Extrusion Solution Team, Tech Center, LG Chem. Ltd., Osan 18126, South Korea; c: Wood Engineering Division, National Institute of Forest Science, Seoul 02455, South Korea;
** Corresponding author: bjkim3@kookmin.ac.kr*

INTRODUCTION

Three-dimensional (3D) printing is a technology that creates real objects by stacking appropriate materials layer-by-layer according to a 3D computer-aided design (Wang *et al.* 2017). This technique is receiving substantial attention as a highly efficient production method alternative for difficult or complex products (Ayrilmis 2018). However, the materials used for 3D printing need to be developed and tested to determine their range, usability, and physical properties of the end products (Utela *et al.* 2008).

Fused deposition modeling (FDM) is currently the most widely used additive manufacturing (AM) technology. The main components of the FDM system include a material feed mechanism, liquefier, print head, gantry, and build surface (Turner *et al.* 2014). When using the FDM method, continuous filaments of thermoplastic polymers are used to 3D print a layer of material. In general, a thin diameter (1.75 or 2.85 mm) filament is heated in a nozzle to reach the semi-liquid state and then extruded onto the platform or the top of the previous output layer. The extruded filaments form a single layer with faces as the head moves on the X-Y plane. The platform on which these layers are stacked moves along the Z axis, and the movement interval of one layer is what determines the Z axis

resolution of the final 3D-printed object. An essential characteristic of this method is the thermoplasticity of the polymer filaments. This is because the filament melts during printing and then solidifies at room temperature within a short time (< 1 s). Its relatively inexpensive cost, high speed, and simplicity are the biggest advantages of the FDM method. However, weak mechanical strength, layer-by-layer appearance, low surface quality, and a limited number of thermoplastic materials are major disadvantages of FDM (Chohan *et al.* 2017).

Wood is a sustainable natural resource that has the advantages of beautiful color, warm texture, and excellent biodegradability; it can be added to the plastic matrix in the form of wood flour to produce biocomposite filaments that are suitable for FDM 3D printing. As a printing material, it can serve as an alternative to the existing 100% plastic material, while at the same time increasing the susceptibility to biodegradation (Wimmer *et al.* 2015). The 3D printing with wood flour is an easy way to use wood resources derived from various kinds of wood and waste wood (logging residue, construction waste wood, *etc.*). Recently, to utilize biomass-based and biodegradable wood materials as feedstock for 3D printing, various studies using wood flour for filament manufacturing are underway. Tao *et al.* (2017) reported that poly lactic acid (PLA) filaments filled with 5 wt% wood flour improved the initial deformation resistance compared to pure PLA. Bi *et al.* (2018) and Guo *et al.* (2018) manufactured filaments by combining wood flour with toughening agents, such as TPU (thermoplastic polyurethane), PCL (polycaprolactone), and POE (poly(ethylene-co-octene)), and then evaluated the mechanical and dynamic properties of the filaments. The cited work demonstrated the potential utility of various combinations of elastomers that offer flexibility and excellent processability.

PLA is characterized by its inherent brittleness and weak impact strength. Hence, the addition of rigid wood flour into PLA matrix results in a lack of toughness. Moreover, the hydrophobic PLA is not compatible with the hydrophilic wood flour (Morreale *et al.* 2008). To overcome these problems, a small amount of maleic anhydride grafted ethylene propylene diene monomer (MA-EPDM), which is widely utilized as an elastomeric polymer, was added to impart durability to the composite material, dampen brittleness, and improve the compatibility between PLA and wood flour (Piontek *et al.* 2020).

In this study, biocomposite filaments were first prepared by commingling PLA, wood flour, and MA-EPDM, and then the morphological, mechanical, and biodegradation properties of the 3D-printed composite specimens were analyzed to ascertain their utility. The objective was to investigate the effects of wood flour on the morphological, mechanical, and biodegradation properties of FDM 3D-printed PLA composites.

EXPERIMENTAL

Materials

The PLA (Ingeo biopolymer 4032D) used in this experiment was provided by Natureworks LLC (Minnetonka, Minnesota, USA). The density, melt flow index, and melting point of the PLA were 1.24 g/cm^3, 2.46 g/10 min (190 °C/2.16 kg), and 155 to 170 °C, respectively. The PLA was used after drying for 48 h at 50 °C before the process input. Wood flour (Arbocel C100) was supplied by J. Rettenmaier & Söhne (Rosenberg, Germany). It mainly consisted of Norway spruce wood (*Picea abies*) with a grain size of 70 to 150 µm and a bulk density of 140 to 180 g/L. Wood flour (WF) was used after drying for 48 h at 105 °C before the process input. Maleic anhydride grafted ethylene propylene

diene monomer (KEPA 1150) was purchased from Kumho Polychem (Seoul, South Korea). The melt index, specific gravity, and maleic anhydride content were 2 g/10 min (230 °C/2.16 kg), 0.88 g/cm^3, and 0.7 wt%, respectively. The MA-EPDM were used after 48 h of drying at 50 °C before the process input.

In the PLA-based composite, WF was added by 10 wt% to 40 wt%, and MA-EPDM was added in a fixed amount of 5 phr to impart elasticity.

Methods

Preparation of composites

Composite materials were melt-compounded using a BA-19 twin screw extruder (Bautek Co., Ltd., Uijeongbu, South Korea) with a length-to-diameter (*L*/*D*) ratio of 40 and 8 temperature zones. The barrel temperature zones of the twin screw extruder was set at 185 °C, 190 °C, 195 °C, 190 °C, 185 °C, 180 °C, 170 °C, and 120 °C, and the extruder rotation speed was 60 rpm. The extruded blends were pelletized using a BA-PLT pelletizer (Bautek Co., Ltd., Uijeongbu, South Korea). The pellets were made into filaments with a diameter of 1.75 mm (± 0.1) using a T-2 single screw extruder (Doldam Tech Co., Gumi, South Korea) with two temperature control sections (210 °C for feeder and 200 °C for die) at the screw speed of 35 rpm. After that, the composite filaments were 3D printed into mechanical specimens (flexural, tensile, and impact) according to ASTM D standards (D256, D638, D790). The 3D printing was carried out using an X1 FDM 3D printer (Hephzibah Co., Ltd., Incheon, South Korea) with a nozzle diameter of 0.6 mm. The 3D-printing temperature and speed were 200 °C and 40 mm/s, respectively. The compounding ratios of the 3D-printed composite specimens are shown in Table 1.

Table 1. Material Designations and Compositions of 3D-printed PLA Composites

Designation	Composition		
	PLA (wt%)	Wood Flour (wt%)	MA-EPDM (phr)
PLA100	100	0	0
PLA/MA-EPDM	100	0	5
WF10	90	10	5
WF20	80	20	5
WF30	70	30	5
WF40	60	40	5

Morphological properties

Field emission scanning electron microscopy (JSM-7401F, JEOL, Tokyo, Japan) was used to investigate the morphological properties of 3D-printed PLA composites with different composition ratios. Specimens were observed to investigate fracture surfaces and 3D-printed laminates after impact strength tests. The specimens were platinum-coated (Sputter Coater 208HR, Cressington Scientific Instruments, Watford, England) after drying for 24 h at 50 °C and then analyzed at an acceleration voltage of 5 or 10 kV.

Mechanical properties

Mechanical tests of the 3D-printed PLA composites were impact strength, tensile properties, and flexural properties. Izod impact strength measurement was carried out using

an impact test machine (DTI-602B, Daekyung Tech, Incheon, South Korea) according to ASTM D256-10 (2018). The tensile and flexural tests were performed using a universal testing machine (H50KS, Tinius Olsen, Horsham, PA, USA) according to ASTM D638-14 (2014) and ASTM D790-17 (2017), respectively. The tensile test speed and the flexural test crosshead speed were all set at 10 mm/min. Ten samples of each specimen were tested and the average values were obtained.

Biodegradation properties

The biodegradability levels of 3D-printed PLA composites with different formulations were tested to evaluate the difference in biodegradability depending on the WF content. The biodegradability test was conducted according to JIS K 1571 (2010). The test method was borrowed and partially modified. The standard specifies two types of fungi to be used as test materials. However, *Fomitopsis palustris*, the brown rot fungus that impacts conifer specimens, was chosen because the WF used for the 3D-printed composites was spruce.

In the biodegradation test, a total of 45 flexural strength specimens were prepared, including 15 for each of the following three formulations: PLA100, WF20, and WF30. In addition to the weight loss that can be attributed to the existing standard methods, the strength loss was also investigated by testing the flexural properties of the fungal-decayed specimen. The flexural strength specimens were dried at 105 ℃ for 48 h in a dry oven to reach a constant weight, and after remaining for 1 h in a desiccator, the weight was measured (0.001 g) and the initial weight was set.

A sterilized plastic net was laid on the pre-cultured fungi, and the specimens were placed on the fungi for 84 d (12 weeks) at a temperature of 26 ℃ ± 2 ℃ and relative humidity of 70%. To examine the trend of weight loss and strength loss, three specimens were selected on the 28^{th} day (4 weeks) and 56^{th} day (8 weeks). When the test was performed after a period of incubation, the hyphae attached to the specimen surface were carefully removed, and then the weight loss was calculated by measuring the weight of the specimen (0.001 g) by drying in an oven at 105 ℃ ± 2 ℃ for 48 h. The flexural strength loss test was carried out using a universal testing machine (H50KS, Tinius Olsen, Horsham, PA, USA) according to ASTM D790-17 (2017), and the test speed was set at 10 mm/min.

RESULTS AND DISCUSSION

Morphological Properties

To investigate the morphological properties of 3D-printed PLA composite specimens with WF and MA-EPDM, the fractured surfaces resulting from impact strength tests as well as the laminated surfaces were examined by field emission scanning electron microscopy (FE-SEM).

The laminated surfaces of the 3D-printed composite made of only PLA are presented in Fig. 1. Each lamination line had a smooth appearance; the division of the laminated surface was clear and uniform. The layer thickness (0.2 mm) was accurately expressed. It was laminated precisely enough to distinguish the print line width and the layer thickness, which were the diameters of the nozzles used for the printing. Moreover, the gap between the boundary line and the bead-shaped edge of each line was confirmed. Figure 1(d) shows the typical wave pattern when brittle fracture occurred. This can confirm

the brittleness of PLA as a morphological characteristic (Martínez-Vázquez *et al.* 2014; Bunkerd *et al.* 2018).

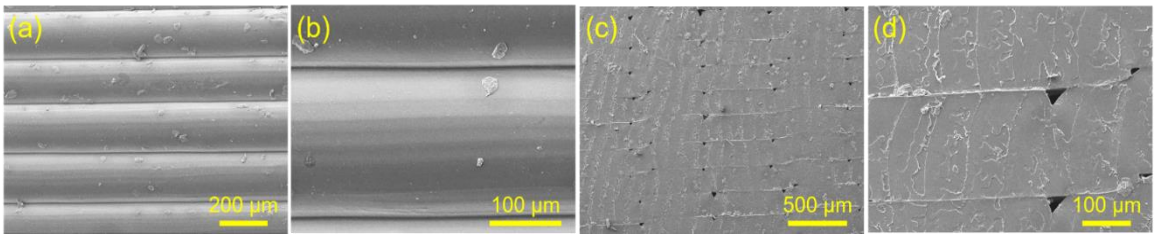

Fig. 1. The SEM images of the layered surfaces: (a) 100×, (b) 300×, and the impact-fractured surfaces: (c) 50×, and (d) 200× of 3D-printed PLA-only composite

Figure 2 shows the 3D-printed PLA composite in which only 5 phr of MA-EPDM was added to PLA. For the lamination surface, the overall appearance was similar to that of pure PLA. However, in contrast to the PLA-only formulation, it was confirmed that EPDM was present in the separated phase protruding at the surface (Pongtanayut *et al.* 2013). It was observed that the EPDM of the dispersed phase stretched in a direction parallel to the printing direction, as opposed to the spherical shape found within a generally incompatible polymer matrix.

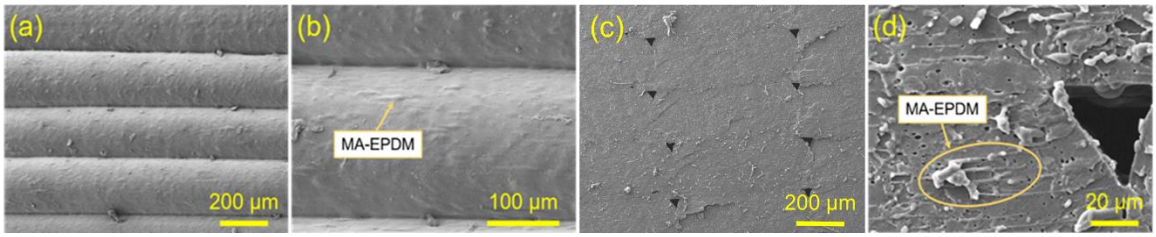

Fig. 2. The SEM images of the layered surfaces: (a) 100×, (b) 300×, and the impact-fractured surfaces: (c) 100×, and (d) 1000× of 3D-printed PLA composite with 5 phr MA-EPDM

The fracture surface was also similar to that of pure PLA. However, as can be seen from the lamination surface, phase-separated MA-EPDM domains were observed on the surface of the PLA matrix. As a result, pores of the same size as the EPDM domain were identified, and it was also confirmed that the EPDM droplets were stretched in the direction of applied force during the impact strength test. This is a new aspect that has not been identified in conventional injection or extrusion molding methods. The FDM technology is characterized by filaments being melt-extruded to form each line, then quickly solidified and laminated. In this process, the printer nozzle moved to form a line, and the speed of moving printer nozzle induced this phenomenon. In typical PLA/EPDM blends, the EPDM is spherical as a result of phase separation due to incompatibility between the two resins (Park *et al.* 2011), but in 3D printing, the spherical EPDM was stretched due to the orientation of the printer nozzle and rapid air cooling. In this regard, it was necessary to conduct further research utilizing other parameters such as printing speed or MA-EPDM content.

From the lamination surface image of the WF10 formulation presented in Fig. 3, the lamination interface was visually confirmed; it was confirmed that the wood flour protruded from the PLA matrix. In addition, it was confirmed that the WF particles were uniformly dispersed through several processes before 3D printing. In the fractured surface

of 3D-printed composite specimen, stacking patterns were not clearly distinguishable, which differed from previous formulations. However, when the images were taken to distinguish one bead, it was found that the size of the WF particle was small or uneven enough to form smooth lines. Additionally, the MA graft-polymerized onto EPDM seemed to bind to the hydroxyl group of the WF, resulting in the EPDM covering the surface of the WF (Oksman and Clemons 1998; Lv *et al*. 2016).

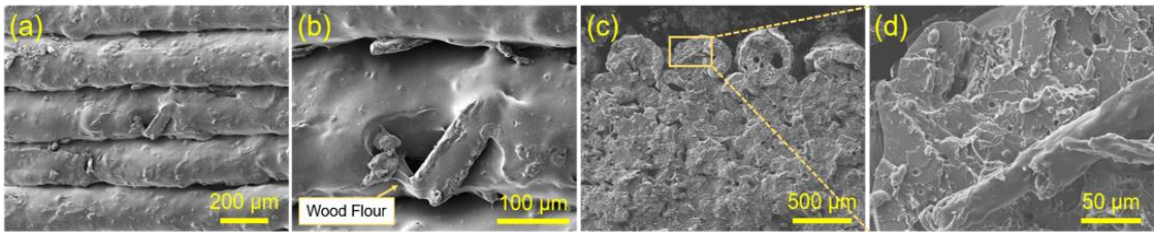

Fig. 3. The SEM images of the layered surfaces: (a) 100×, (b) 300×, and the impact-fractured surfaces: (c) 50×, and (d) 500× of 3D-printed PLA composite with 5 phr MA-EPDM and 10 wt% WF

For the laminated surface of the WF20 formulation presented in Figs. 4(a) and 4(b), the division at the laminated interface became irregular and the frequency of protruding wood flour from the surface increased. For the fracture surface shown in Figs. 4(c) and 4(d), it was more difficult to distinguish the lamination patterns, and it was confirmed that the presence of EPDM-coated WF in the PLA matrix inhibited the interfacial bonding.

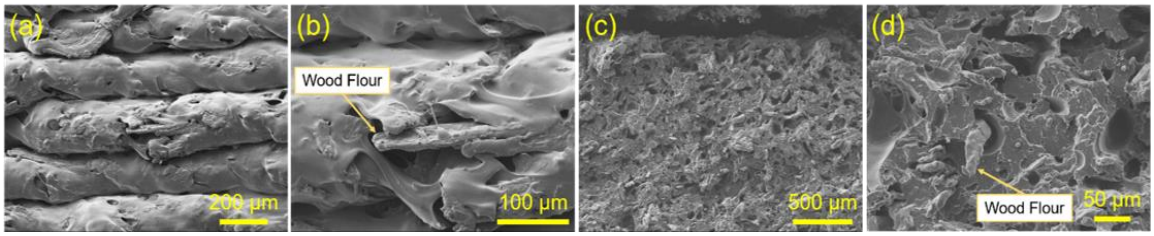

Fig. 4. The SEM images of the layered surfaces: (a) 100×, (b) 300×, and the impact-fractured surfaces: (c) 50×, and (d) 300× of 3D-printed PLA composite with 5 phr MA-EPDM and 20 wt% WF

Figure 5 shows the SEM images of composites with WF30. As the WF content was increased to 30 wt%, the protruding WF particles increased and the presence of such WF hindered the formation of the PLA matrix lines. This led to the increased number of voids on the surface, and this tendency was observed in both the laminated and fracture surfaces.

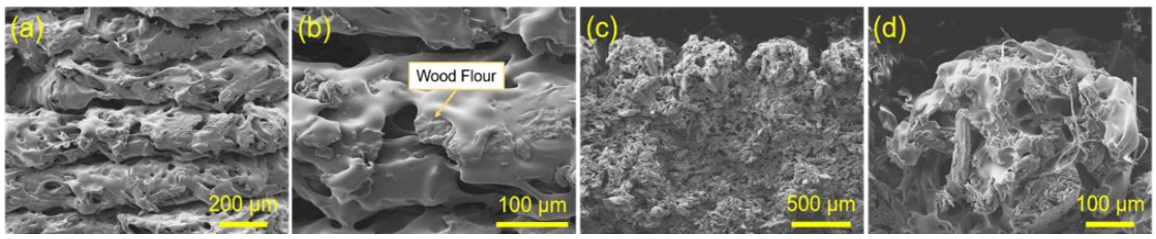

Fig. 5. SEM images of the layered surfaces: (a) 100×, (b) 300×, and the impact-fractured surfaces: (c) 50×, and (d) 200× of 3D-printed PLA composite with 5 phr MA-EPDM and 30 wt% WF

In the laminated surface of the WF40 formulation as shown in Fig. 6, the boundary of the laminated interface was completely destroyed and the entire surface was irregular and very rough.

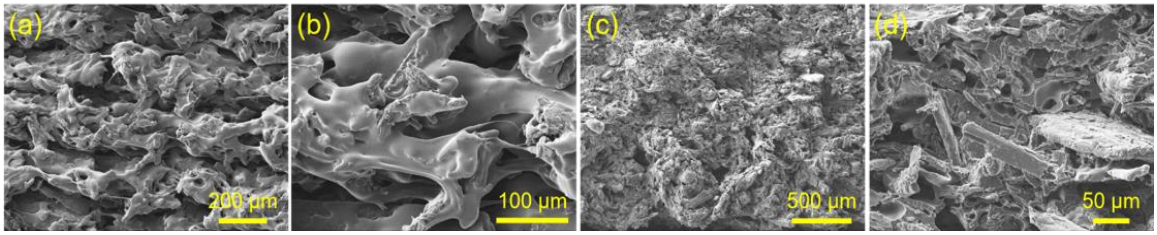

Fig. 6. SEM images of the layered surfaces: (a) 100×, (b) 300×, and impact-fractured surfaces: (c) 50×, and (d) 300× of 3D-printed PLA composite with 5 phr MA-EPDM and 40 wt% WF

Through observing the morphological properties, it was confirmed that the voids were present in all formulations with WF. The voids were caused by the addition of WF, and the model of the void generation mechanism was presented. The scheme of the model is shown in Fig. 7.

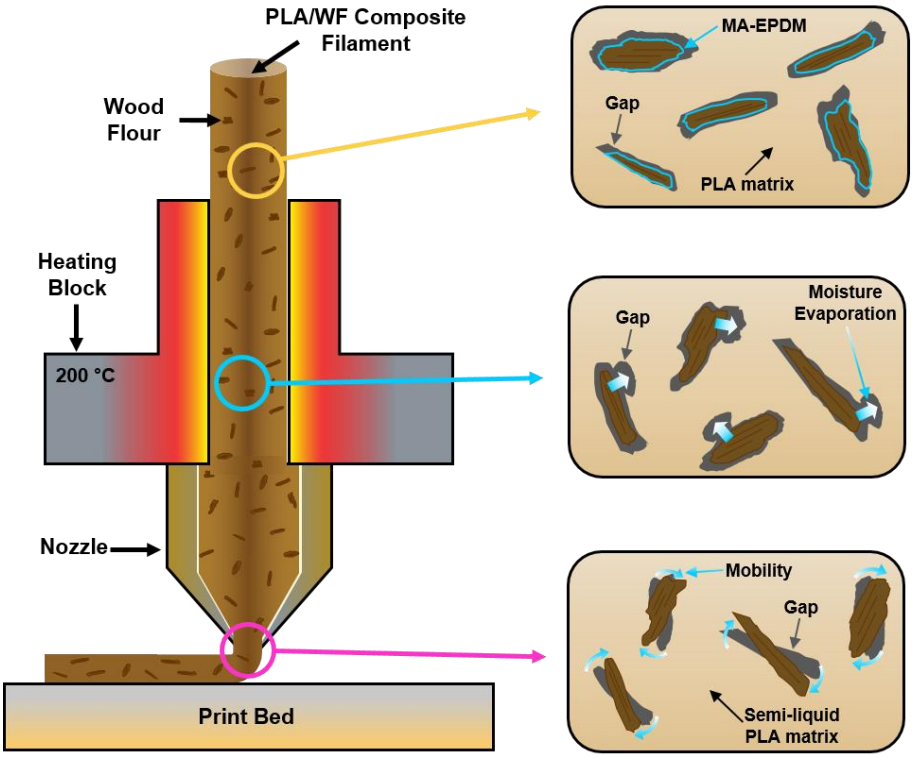

Fig. 7. Void generation mechanism models caused by WF addition

The first reason for the voids was the incompatibility between MA-EPDM and PLA. A small amount (*i.e.*, 5 phr) of MA-EPDM was added to compensate for the high stiffness of PLA and WF. However, it was confirmed by the morphological property analysis that the MA component graft-polymerized onto EPDM preferentially binds to the hydroxyl group of WF and consequently covers the WF like a coating (Lv *et al.* 2016).

Therefore, due to the incompatibility between the EPDM coverings on the surface of the WF and PLA, it can be surmised that the voids were caused by the addition of WF.

The second rationale was that the moisture in the WF evaporated when the filament was heated. The WF is a high moisture content material. Therefore, when it is made into filament and stored, it absorbs moisture in the atmosphere. When the filament is melted at approximately 200 °C, due to the rapid increase in temperature, the moisture in the WF vaporizes and is discharged out of the WF, pushing out the polymer matrix in the melt flow state and creating a spatial volume (Joshi and Marathe 2010). The voids generated by this activity are relatively small in size and irregular.

The third component of void formation was due to the movement of the WF. When a high temperature of approximately 200 °C was applied to the filament, the polymer melted and existed in a semi-liquid state. However, because the main component of the WF was cellulose, WF did not undergo a phase change and continued to exist in a solid state. In this state, when the filament was extruded from the nozzle, the WF maintained its rigidity despite the movement. The semi-liquid polymer was exposed to the atmosphere and cured. At this time, the space generated by the movement of the WF was not filled and the voids hardened. All of these void generation mechanisms occurred in this test. Voids can be seen in both laminate and fracture surfaces from the SEM images. The generation of such voids may affect the mechanical property and biodegradability of the composites.

Mechanical Properties

The tensile strength, tensile modulus, elongation at break, and impact strength of 3D-printed PLA composite specimens are shown in Fig. 8.

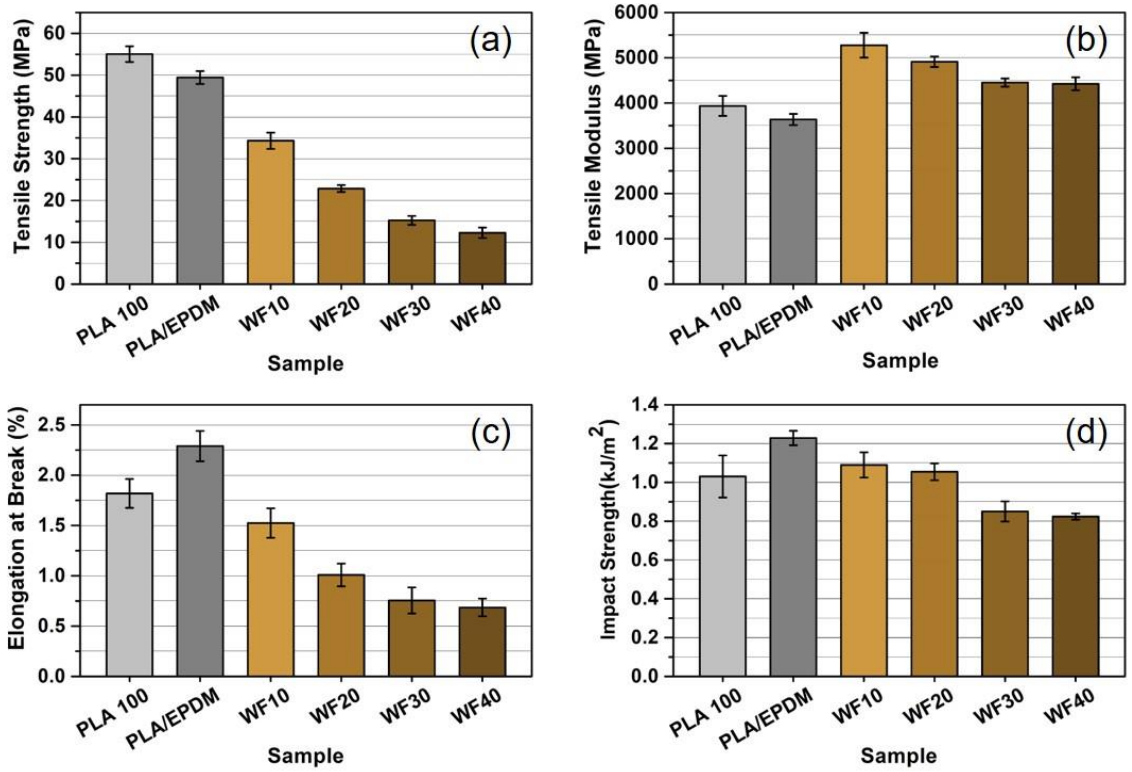

Fig. 8. Tensile properties and impact strength of 3D-printed PLA composites as a function of wood flour content: (a) tensile strength, (b) tensile modulus, (c) elongation at break, and (d) impact strength

In the case of tensile modulus, the value increased remarkably after the addition of WF. However, as the amount of WF increased, the tensile modulus tended to decrease. However, even at 40 wt% of the maximum amount of WF, it remained 15% higher than pure PLA. This was the result of the increase in the stiffness of the composite as the wood, which has excellent stiffness, was added (Kariz *et al.* 2018). In contrast, when 5 phr of MA-EPDM was added to pure PLA, ductility was improved in PLA and the value decreased slightly.

In the case of elongation at break, the addition of MA-EPDM increased its value by giving the composite viscoelasticity. However, the value decreased rapidly as WF was added. Tensile strength decreased slightly when MA-EPDM was added to pure PLA. This was because the increased viscoelasticity by EPDM led to the decreased maximum stress tolerance of PLA. As WF was added, the tensile strength tended to decrease. However, when the reduced value was compared to that of polypropylene (PP), one popular plastic, it has an equivalent value up to 20 wt% of WF content, which indicated a sufficient use range in application (Kerbow and Mark 1999).

An inherent drawback of PLA is its brittleness. It is vulnerable to impact and easily broken or cracked. However, the impact strength of PLA was improved by the addition of EPDM elastomer. Furthermore, even when WF was added up to 20 wt%, the impact strength was higher than that of pure PLA. When WF was added more than 30 wt%, the impact strength value was lower than that of pure PLA (Daver *et al.* 2018).

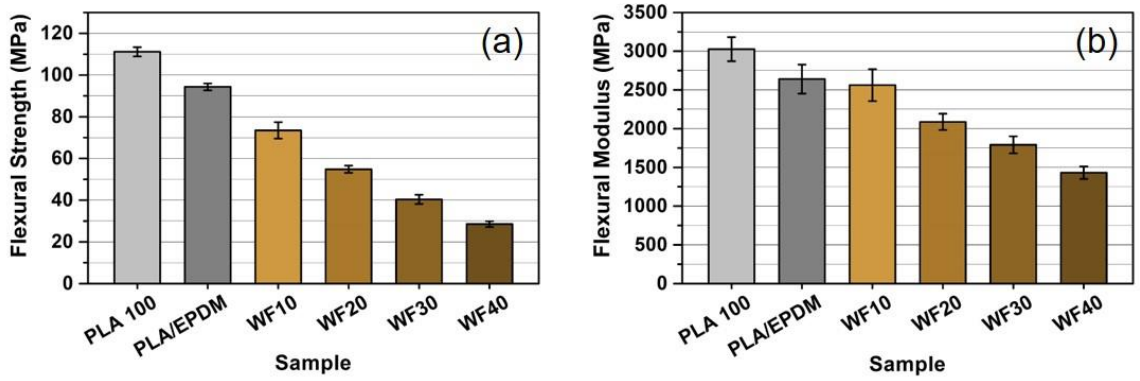

Fig. 9. Flexural properties of 3D-printed PLA composites as a function of wood flour content: (a) flexural strength and (b) flexural modulus

As shown in Fig. 9, both the flexural strength and flexural modulus were slightly decreased when EPDM was added; both decreased with the addition of WF. The addition of MA-EPDM and WF to PLA had a negative effect on its flexural properties. However, PLA is a robust material with strong inherent flexural properties. Hence, the 3D-printed PLA composites with MA-EPDM and WF (up to 40 wt%) had a higher flexural modulus compared to PP (Kerbow and Mark 1999). The above results showed that the mechanical properties of 3D-printed PLA composites did not present an obstacle in real applications.

Biodegradation Properties

Biodegradation tests for PLA, WF20, and WF30 formulations were carried out to analyze the biodegradability of PLA composites filled with wood flour by weight loss and strength loss. In addition, photographs were taken under the same conditions for visual observation; and during the biodegradation test, the analyses for the growth of fungi on the

specimens in culture bottles were conducted at intervals of 7 d. Photographs of the specimens are shown in Fig. 10.

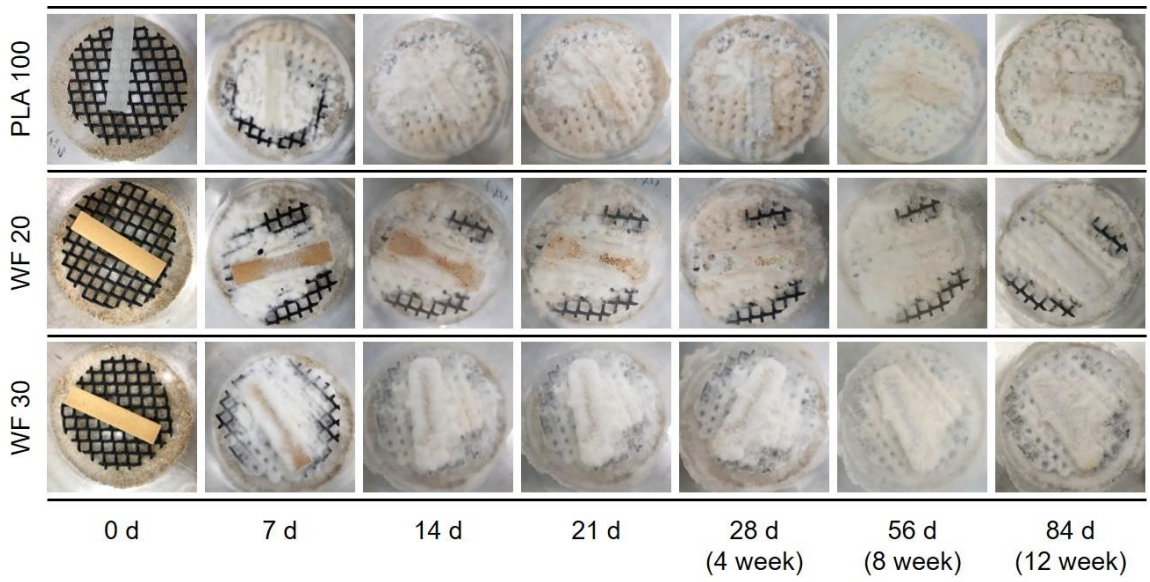

Fig. 10. Colonization of *Fomitopsis palustris* on 3D-printed PLA composites after biological degradation according to wood flour content over 12 weeks

After starting the biodegradation test, mycelia of brown rot fungus were grown in plastic nets and confirmed in all formulations. Seven days after the start of the test, the hyphae reached the specimens rapidly and extended the growth, especially in the WF-added formulation. In terms of wood flour content, the hyphae of the WF30 composite with an additional 10 wt% wood flour covered the upper part of the specimen, showing more pronounced activity than the WF20 composite. This pattern was similar to that seen in the week 4 test, but by week 4, the authors observed that mycelia covered the specimens at similar levels in all formulations, including the PLA formulation. In addition, it covered the plastic net and the sand, and it was confirmed that the mycelium had nutrient growth activity. At about 8 weeks after the biodegradation test, no clear difference was observed between the hyphae in the culture bottle. However, the upper part of the specimen was covered with a thicker layer. The mycelium of brown rot fungus gradually darkened in shade, but it did not show a distinct difference until week 12. Visual observation of the specimens in the culture bottle confirmed that there was a difference in the initial mycelial growth rate between each formulation. In addition, even in the PLA mixture without any WF, the mycelia were able to grow rapidly from the beginning to cover the specimen, indicating that the PLA polymer can be compatible with biodegradation conditions and did not interfere with the growth of fungi.

SEM images of the surface of 3D-printed PLA composite filled with 30 wt% WF after 12 weeks of biodegradation tests are shown in Fig. 11. Since hyphae were removed from the surface to measure weight and strength losses, the hyphae could not be found on the outermost surface, but the hyphae were found inside the pores of the composite surface. The presence of pores caused by WF seemed to play an important role in the availability of space for microorganisms to grow. Therefore, traces of active microbial growth were found in almost all voids. The mycelia were attached to and grown on the surface of PLA polymer as well as WF.

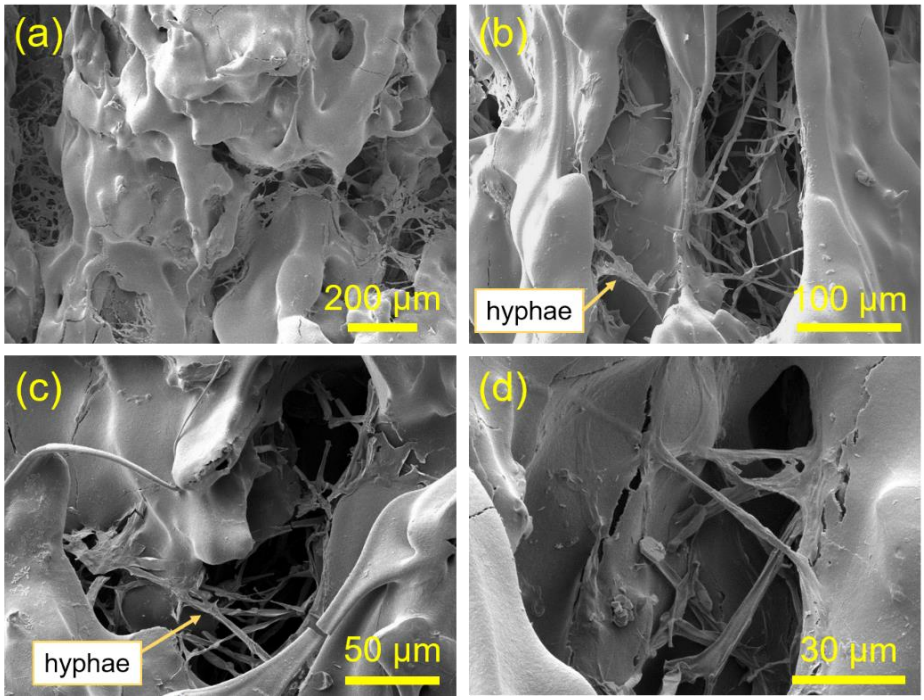

Fig. 11. SEM images of 3D-printed PLA composite surface (*i.e.*, WF30 specimen) after biodegradation test for 12 weeks: (a) ×100, (b) ×300, (c) ×500, and (d) ×1,000

The SEM images after the biodegradation test confirmed not only the presence of the hyphae but also the degradation of the PLA polymer. During the biodegradation test, it was considered that the 3D-printed PLA composites were exposed to high humidity and the hydrolysis of the PLA polymer occurred actively (Ndazi and Karlsson 2011; Lee *et al.* 2014). Therefore, it can be seen from Figs. 11(c) and 11(d) that there are frequent cracks on the composite surface. In addition, it was considered that tension was generated as the hyphae adhered to the inner surface of the pore, and then, as the wetting and drying process was repeated, thereby promoting crack generation on the composite surface.

The active growth of the hyphae, which can be seen in the SEM images, and the degradation resulted from the hydrolysis of PLA polymer mainly affected the weight loss and strength loss of the 3D-printed PLA composites.

The weight loss and the strength loss measurements were obtained by taking out three specimens from each group after 4 weeks and 8 weeks to identify the weight and the strength decreases. At week 12, at the end of the biodegradation test, the weight loss and strength loss of nine specimens were calculated according to the following Eqs. 1 and 2,

$$\text{Weight Loss } (\%) = \frac{W_\text{i} - W_\text{f}}{W_\text{i}} \times 100 \quad (1)$$

where W_i is the initial weight (g) of the oven-dried specimen before the biodegradation test and W_f is the final weight (g) of the oven-dried specimen after the biodegradation test,

$$\text{Strength Loss } (\%) = \frac{S_\text{i} - S_\text{f}}{S_\text{i}} \times 100 \quad (2)$$

where S_i is the initial strength (MPa) of the oven-dried specimen before the biodegradation test and S_f is the final strength (MPa) of the oven-dried specimen after the biodegradation test.

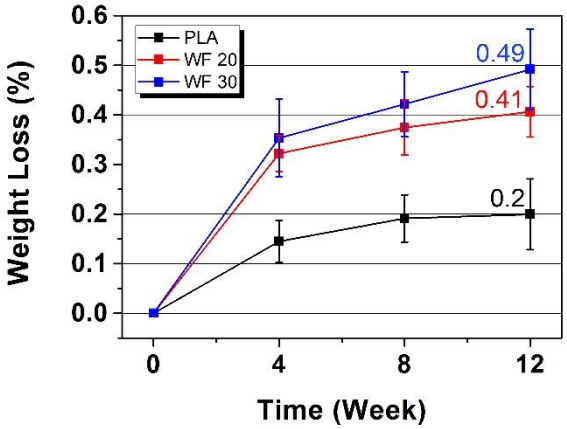

Fig. 12. Weight loss of 3D-printed PLA composites by biodegradation

Figure 12 represents a 12-week biodegradation test result showing weight loss across all formulations. This test showed a rapid growth of hyphae at the beginning of the biodegradation test, the invasion of hyphae into the specimen, and the degradation of components by microorganisms within both WF and PLA. Moreover, the degree of biodegradation during the test period can be determined by the slope of the graph progressed up to week 12. When WF was added, the weight loss increased more than 0.3% within 4 weeks. After that, the weight loss progressed by about 0.1% until the end of the final test. This meant that the hyphae covered the surface of the composite specimen quickly at the beginning of the test and at the same time grew by using the WF as their nutrient source. This phenomenon was more prominent in the WF30 blend with 10 wt% more wood flour, resulting in greater weight loss due to fungal decay. This was because brown rot fungus grew by using the cellulose component as a nutrient source; the cellulose is the most important constituent of WF, compared to the organic chain of PLA polymer (Xu and Goodell 2001). This may be supported by comparing with the weight loss seen in PLA, because the PLA-WF formulations (WF20 and WF30) showed more than twice the weight loss rate of the PLA-only formulation in all periods. Nevertheless, meaningful weight loss through the biodegradation test occurred in the PLA-only formulation. This meant that even if the PLA polymer did not act as a direct nutrient source for the growth of fungi, the mycelium were able to expand spatially with growth metabolism and consequently, the mycelium covered the surface of the specimen. The conditions for the test were very warm and humid at temperatures of approximately 26 ℃ and more than 70% relative humidity, and the surface of specimens covered by the mycelium were maintained at a high humidity. At this time, it is well known that PLA stored at high humidity experiences surface degradation; *i.e.*, molecular weight degradation and cracks occur as a result of hydrolysis on the surface of PLA (Paul *et al.* 2005; Elsawy *et al.* 2017). Therefore, it can be seen that the hydrolysis between the polymer chains of PLA occurred actively during the biodegradation test at high relative humidity conditions. Furthermore, microscopic voids existed between layers due to the nature of 3D-printed composites filled with WF. Compared to conventional composite materials, 3D-printed composites had a relatively high specific surface area due to their high porosity, so they had abundant surfaces that mycelium can penetrate. This evidence seemed to point clearly to the cause of weight loss.

Nevertheless, when compared to other research on the biodegradation of composites prepared using PE or PLA as a matrix and adding 20 wt% to 30 wt% of WF or sawdust, the weight loss value is not high enough to support the above-mentioned phenomenon (Tazi *et al.* 2018; Candelier *et al.* 2019). The reason had to do with the morphological properties. The WF protruding from the surface of the specimen, which is thought to be the primary source of nutrients for the mycelia, was covered with MA-EPDM. Therefore, the pure WF surface that the mycelia could come in contact with was noticeably reduced. The reason for the higher weight loss in the WF30 formulation was the presence of larger amounts of wood flour. In addition, the amount of supplemental MA-EPDM was fixed at 5 phr even when the amount of WF increased. Because the amount of MA-EPDM that can bind to the surface of the protruding WF was set, the higher the WF content, the higher the amount of protruding WF. As a result, the amount of MA-EPDM coating the WF surface was reduced, thereby increasing the amount and frequency of pure WF that can be exposed at the surface. Accordingly, the fungus primarily degraded the surface of the pure WF, which was thought to lead to greater weight loss. Additionally, it was thought that the mass losses were from hydrolysis of the PLA polymer matrix due to frequent moisture interference (dampening and drying) during the hyphae removal coming from the test procedures.

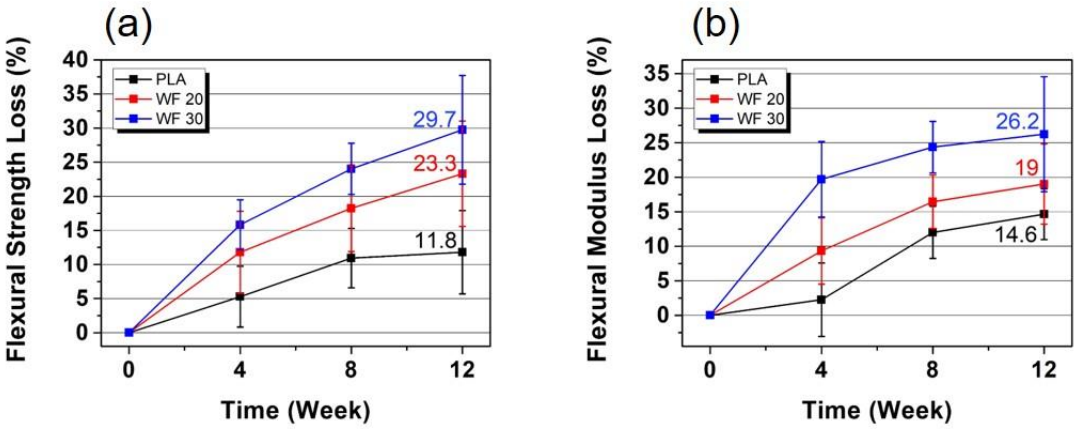

Fig. 13. Strength loss of 3D-printed PLA composites by biodegradation: (a) flexural strength loss and (b) flexural modulus loss

Figure 13 shows that there was a loss in flexural strength and modulus for all formulations after biodegradation tests over 12 weeks (Schirp *et al.* 2008). The difference between the blends was similar to that of the weight loss, which was higher in both the WF20 and WF30 blends with wood flour than in the PLA blend without the wood flour; the higher wood flour content resulted in the greater strength loss. This was demonstrated by the rapid mass loss during the first 4 weeks. Among the components of WF, cellulose acted as a structural support, giving WF high rigidity. This cellulose component was lost, as it provided the main nutrient source for brown rot fungi, which destroyed the structure of the WF and reduced the mass. Additionally, the WF, which acted as a stress transporter between PLA polymers, deteriorated, and its stiffness was noticeably decreased. Thus, the flexural stress of composite filled with WF decreased considerably. This phenomenon was more clearly seen in 3D-printed composites with high porosity and specific surface area because hyphae can infiltrate the pores inside the specimen to degrade protruding WF.

There was a potential for greater biodegradation compared to conventional plastic/WF composites prepared with molding processes (Schultz 2008). In addition, during the test process, water saturation and drying processes were frequently performed; hydrolysis occurred in the PLA matrix, which was a common substrate of each formulation. The addition of WF led to a greater amount of moisture saturation, causing the specimen to bend or warp. Hence, greater dimensional deformation occurred, which was also considered to be the cause of the remarkably lowered mechanical properties demonstrated in the flexural strength test (Schirp and Wolcott 2005). For these reasons, it is believed that the PLA mixture without WF showed meaningful weight loss and strength loss.

CONCLUSIONS

1. Based on polylactic acid (PLA) matrix, wood flour (WF) was added to fused deposition modeling (FDM) 3D printing filaments, and 3D-printed to prepare a composite material. As a result of the morphological analysis, it was confirmed that the maleic anhydride grafted ethylene propylene diene monomer (MA-EPDM) of the separated phase was stretched due to the speed during the FDM 3D-printing process. Adding WF to the PLA polymer generated voids that hindered the formation of a printing line. As the amount of WF increased, the frequency of void generations increased and the size of the voids also increased, which resulting in a decrease in overall 3D printing quality.
2. Due to the generation of voids, the density of the 3D-printed PLA composite was reduced, and as the WF was added, the mechanical strength was degraded. However, the addition of MA-EPDM for elasticity demonstrated favorable changes in elongation and impact strength. Mechanism models to account for void generation resulting from the addition of WF were presented and discussed.
3. The addition of WF to the composite formulations resulted in higher weight loss and strength loss in the biodegradation test results. This suggested that the addition of wood flour improved the biodegradation properties of 3D-printed PLA composites, making them more environmentally friendly. The composites can be used as a resource-recycling material.

ACKNOWLEDGMENTS

This study was carried out with the support of 'R&D Program for Forest Science Technology (Project No. 2019150B10-2123-0301)' provided by Korea Forest Service (Korea Forestry Promotion Institute) and the National Institute of Forest Science (Project No. A2019-0149).

REFERENCES CITED

ASTM D256-10 (2018). "Standard test methods for determining the Izod pendulum impact resistance of plastics," ASTM International, West Conshohocken, PA. DOI: 10.1520/D0256-10R18

ASTM D638-14 (2014). "Standard test method for tensile properties of plastics," ASTM International, West Conshohocken, PA. DOI: 10.1520/D0638-14

ASTM D790-17 (2017). "Standard test methods for flexural properties of unreinforced and reinforced plastics and electrical insulating materials," ASTM International, West Conshohocken, PA, DOI: 10.1520/D0790-17

Ayrilmis, N. (2018). "Effect of layer thickness on surface properties of 3D printed materials produced from wood flour/PLA filament," *Polym. Test.* 71, 163-166. DOI: 10.1016/j.polymertesting.2018.09.009

Bi, H. H., Ren, Z. C., Guo, R., Xu, M., and Song, Y. M. (2018). "Fabrication of flexible wood flour/thermoplastic polyurethane elastomer composites using fused deposition molding," *Ind. Crop. Prod.* 122, 76-84. DOI: 10.1016/j.indcrop.2018.05.059

Bunkerd, R., Molloy, R., Somsunan, R., Punyodom, W., Topham, P. D., and Tighe, B. J. (2018). "Synthesis and characterization of chemically-modified cassava starch grafted with poly (2-ethylhexyl acrylate) for blending with poly (lactic acid)," *Starch* 70(11-12), article ID 1800093. DOI: 10.1002/star.201800093

Candelier, K., Atli, A., and Alteyrac, J. (2019). "Termite and decay resistance of bioplast-spruce green wood-plastic composites," *Eur. J. Wood Wood Prod.* 77, 157-169. DOI: 10.1007/s00107-018-1368-y

Chohan, J. S., Singh, R., Boparai, K. S., Penna, R., and Fraternali, F. (2017). "Dimensional accuracy analysis of coupled fused deposition modeling and vapour smoothing operations for biomedical applications," *Compos. Part B- Eng.* 117, 138-149. DOI: 10.1016/j.compositesb.2017.02.045

Daver, F., Lee, K. P. M., Brandt, M., and Shanks, R. (2018). "Cork–PLA composite filaments for fused deposition modelling," *Compos. Sci. Technol.* 168, 230-237. DOI: 10.1016/j.compscitech.2018.10.008

Elsawy, M. A., Kim, K. H., Park, J. W., and Deep, A. (2017). "Hydrolytic degradation of polylactic acid (PLA) and its composites," *Renew. Sustain. Energy Rev.* 79, 1346–1352. DOI: 10.1016/j.rser.2017.05.143

Guo, R., Ren, Z. C., Bi, H. J., Song, Y. M., and Xu, M. (2018). "Effect of toughening agents on the properties of poplar wood flour/poly (lactic acid) composites fabricated with fused deposition modeling," *Eur. Polym. J.* 107, 34-45. DOI: 10.1016/j.eurpolymj.2018.07.035

JIS K 1571 (2010). "Wood preservatives - Performance requirements and their test methods for determining effectiveness." Japanese Standards Association, Tokyo, Japan

Joshi, P. S., and Marathe, D. S. (2010). "Mechanical properties of highly filled PVC/wood-flour composites," *J. Reinf. Plast. Compos.* 29(16), 2522–2533. DOI: 10.1177/0731684409353815

Kariz, M., Sernek, M., Obućina, M., and Kuzman, M. K. (2018). "Effect of wood content in FDM filament on properties of 3D printed parts," *Mater. Today Commun.* 14, 135–140. DOI: 10.1016/j.mtcomm.2017.12.016

Kerbow, D., and Mark, J. (1999). *Polymer Data Handbook*, Oxford University Press Inc., Oxford, UK.

Lee, S. H., Kim, I. Y., and Song, W. S. (2014). "Biodegradation of polylactic acid (PLA) fibers using different enzymes," *Macromol. Res.* 22(6), 657-663. DOI: 10.1007/s13233-014-2107-9

Lv, S. S., Gu, J. Y., Tan, H. Y., and Zhang, Y. H. (2016). "Modification of wood flour/PLA composites by reactive extrusion with maleic anhydride," *J. Appl. Polym. Sci.* 133(15), article ID 43295. DOI: 10.1002/app.43295

Martínez-Vázquez, F. J., Pajares, A., Guiberteau, F., and Miranda, P. (2014). "Effect of polymer infiltration on the flexural behavior of β-tricalcium phosphate robocast scaffolds," *Materials* 7(5), 4001-4018. DOI: 10.3390/ma7054001

Morreale, M., Scaffaro, R., Maio, A., and La Mantia, F. P. (2008). "Effect of adding wood flour to the physical properties of a biodegradable polymer," *Compos. Part A-Appl. S.* 39(3), 503-513. DOI: 10.1016/j.compositesa.2007.12.002

Ndazi, B. S., and Karlsson, S. (2011). "Characterization of hydrolytic degradation of polylactic acid/rice hulls composites in water at different temperatures," *Express Polym. Lett.* 5(2), 119-131. DOI: 10.3144/expresspolymlett.2011.13

Oksman, K., and Clemons, C. (1998). "Mechanical properties and morphology of impact modified polypropylene-wood flour composites," *J. Appl. Polym. Sci.* 67(9), 1503-1513. DOI: 10.1002/(SICI)1097-4628(19980228)67:9<1503::AID-APP1>3.0.CO;2-H

Park, D. H., Kim, M. S., Yang, J. H., Lee, D. J., Kim, K. N., Hong, B. K., and Kim, W. N. (2011). "Effects of compatibilizers and hydrolysis on the mechanical and rheological properties of polypropylene/EPDM/poly (lactic acid) ternary blends," *Macromol. Res.* 19(2), 105-112. DOI: 10.1007/s13233-011-0215-3

Paul, M. A., Delcourt, C., Alexandre, M., Degée, P., Monteverde, F., and Dubois, P. (2005). "Polylactide/montmorillonite nanocomposites: Study of the hydrolytic degradation," *Polym. Degrad. Stab.* 87(3), 535-542. DOI: 10.1016/j.polymdegradstab.2004.10.011

Piontek, A., Vernaez, O., and Kabasci, S. (2020). "Compatibilization of poly (lactic acid) (PLA) and bio-based ethylene-propylene-diene-rubber (EPDM) *via* reactive extrusion with different coagents," *Polymers* 12(3), article no. 605. DOI: 10.3390/polym12030605

Pongtanayut, K., Thongpin, C., and Santawitee, O. (2013). "The effect of rubber on morphology, thermal properties and mechanical properties of PLA/NR and PLA/ENR blends," *Energy Procedia* 34, 888-897. DOI: 10.1016/j.egypro.2013.06.826

Schirp, A., Ibach, R. E., Pendleton, D. E., and Wolcott, M. P. (2008) "Biological degradation of wood-plastic composites (WPC) and strategies for improving the resistance of WPC against biological decay," in: *Development of Commercial Wood Preservatives,* ACS Publications, Washington, D.C., USA, pp. 480-507.

Schirp, A., and Wolcott, M. P. (2005). "Influence of fungal decay and moisture absorption on mechanical properties of extruded wood-plastic composites," *Wood Fiber Sci.* 37(4), 643-652.

Schultz, T. P. (2008). *Development of Commercial Wood Preservatives*, American Chemical Society, Washington, D.C., USA.

Tao, Y. B., Wang, H. L., Li, Z. L., Li, P., and Shi, S. Q. (2017). "Development and application of wood flour-filled polylactic acid composite filament for 3D printing," *Materials* 10(4), article no. 339. DOI: 10.3390/ma10040339

Tazi, M., Erchiqui, F., and Kaddami, H. (2018). "Influence of softwood-fillers content on the biodegradability and morphological properties of wood-polyethylene composites," *Polym. Compos.* 39(1), 29-37. DOI: 10.1002/pc.23898

Turner, B. N., Strong, R., and Gold, S. A. (2014). "A review of melt extrusion additive manufacturing processes: I. Process design and modeling," *Rapid Prototyping J.* 20(3), 192-204. DOI: 10.1108/RPJ-01-2013-0012

Utela, B., Storti, D., Anderson, R., and Ganter, M. (2008). "A review of process development steps for new material systems in three dimensional printing (3DP)," *J. Manuf. Process.* 10(2), 96-104. DOI: 10.1016/j.jmapro.2009.03.002

Wang, X., Jiang, M., Zhou, Z., Gou, J., and Hui, D. (2017). "3D printing of polymer matrix composites: A review and prospective," *Compos. Part B- Eng.* 110, 442-458. DOI: 10.1016/j.compositesb.2016.11.034

Wimmer, R., Steyrer, B., Woess, J., Koddenberg, T., and Mundigler, N. (2015). "3D printing and wood," *Pro Ligno* 11(4), 144-149.

Xu, G., and Goodell, B. (2001). "Mechanisms of wood degradation by brown-rot fungi: Chelator-mediated cellulose degradation and binding of iron by cellulose," *J. Biotechnol.* 87(1), 43-57. DOI: 10.1016/s0168-1656(00)00430-2

Article submitted: September 16, 2020; Peer review completed: February 13, 2021; Revised version received and accepted: August 27, 2021; Published: September 9, 2021.
DOI: 10.15376/biores.16.4.7122-7138